

V729 Sgr: A long period dwarf nova showing negative superhumps during quiescence

Gavin Ramsay¹, Matt A. Wood², John K. Cannizzo^{3,4}, Steve B. Howell⁵, Alan Smale⁶

¹*Armagh Observatory & Planetarium, College Hill, Armagh, BT61 9DG, UK*

²*Department of Physics and Astronomy, Texas A&M University–Commerce, Commerce, TX 75429, USA*

³*CRESST and Astroparticle Physics Laboratory NASA/GSFC, Greenbelt, MD 20771, USA*

⁴*Department of Physics, University of Maryland, Baltimore County, 1000 Hilltop Circle, Baltimore, MD 21250, USA*

⁵*NASA Ames Research Center, Moffett Field, CA 94095, USA*

⁶*NASA Goddard Space Flight Center, Greenbelt, MD 20771, USA*

Accepted 2017 April 4. Received 2017 April 4; in original form 2017 February 17

ABSTRACT

We report *K2* observations of the eclipsing cataclysmic variable V729 Sgr which covered nearly 80 days in duration. We find five short outbursts and two long outbursts, one of which shows a clear plateau phase in the rise to maximum brightness. The mean time between successive short outbursts is ~ 10 d while the time between the two long outbursts is ~ 38 d. The frequency of these outbursts are unprecedented for a CV above the orbital period gap. We find evidence that the mid-point of the eclipse occurs systematically earlier in outburst than in quiescence. During five of the six quiescent epochs we find evidence for a second photometric period which is roughly 5 percent shorter than the 4.16 h orbital period which we attribute to negative superhumps. V729 Sgr is therefore one of the longest period CVs to show negative superhumps during quiescence.

Key words: accretion, accretion discs – stars: dwarf novae – stars: individual: V729 Sgr – novae, cataclysmic variables

1 INTRODUCTION

After the second of the *Kepler* satellite’s reaction wheels failed in May 2013, the space mission was re-purposed and renamed *K2*. Unlike the original mission which continuously monitored a 115 square degree field north of the Galactic plane between Cygnus and Lyra for 4 years, *K2* monitors fields along the ecliptic plane, each pointing lasting ~ 70 – 80 days (see Howell et al. 2014). *K2* has been used to study a wide variety of astronomical sources including exoplanets, galaxies, solar system objects, and cataclysmic variables (e.g., Dai et al. 2016; Kennedy et al., 2016).

Briefly, cataclysmic variables (CVs) are interacting binaries in which a low mass star (typically a K/M dwarf) fills its Roche lobe and the material which flows through the L1 point forms an accretion disk around the more massive white dwarf (if the white dwarf has a magnetic field $\gtrsim 1$ MG the disk is either partially or completely prevented from forming). In the dwarf-novae sub-class of CVs, eruptions are seen every few weeks or months where the brightness of the system increases by ~ 1 – 5 mag. These outbursts, arising from instabilities in the accretion disk, are excellent sources with which to study the physics of interacting binaries and accretion processes.

K2 observations during Campaign 9¹ took place towards the end of 2015 and one of the sources observed was EPIC 214539533, the CV V729 Sgr. This star was first identified as being variable in 1928 with further observations made by Ferwerda (1934) showing it to be an irregular variable with successive maxima being separated by 12–17 days. Although being fairly bright ($V \sim 14$ during outburst), V729 Sgr has not been particularly well studied, apart from that of Cieslinski et al. (2000). These authors confirmed its CV nature and found that V729 Sgr was an eclipsing system with a period of 4.16 hrs. In this paper, we report on the *K2* observations of V729 Sgr.

2 OVERVIEW OF THE *K2* OBSERVATIONS

K2 observations of V729 Sgr were made between MJD = 57301.0–57382.4 (2015 Oct 5 – 2015 Dec 26) and were obtained in Short Cadence (SC) mode which yields an effective exposure time of 58.8 sec. Since the *K2* raw light curves of sources need to be photometrically corrected for instrumental effects caused by minute changes to its pointing (van

¹ <https://keplerscience.arc.nasa.gov/k2-fields.html>

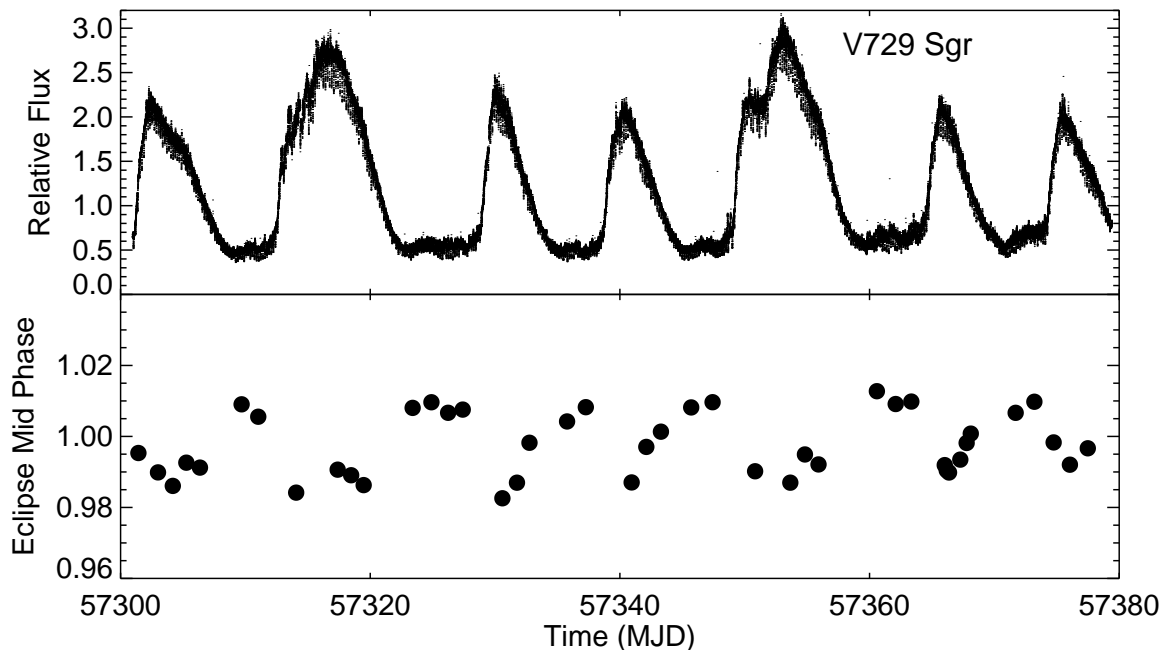


Figure 1. Top Panel: The K2 short cadence light curve of V729 Sgr. Lower panel: the orbital phase of the eclipse where 6–8 successive eclipses have been averaged to determine the eclipse mid-point.

Cleve et al., 2016), Andrew Vanderburg very kindly supplied the corrected SC light curve using the techniques outlined in Vanderburg & Johnson (2014).

We show the light curve of V729 Sgr in the top panel of Figure 1 and note that it is characteristic of a CV showing regular outbursts. There are seven outbursts, two of which have higher peak fluxes and significantly longer duration than the other five: we call these ‘long’ outbursts and the others ‘short’ outbursts. On average there is an outburst every 12.7 d, with short outbursts lasting ~ 6.4 d and long lasting ~ 10.4 d. The mean time interval between successive short outbursts is 10.0 d and the time interval between the two long outbursts is ~ 38 days. The orbital period of V729 Sgr (4.16 h) is similar to that of the prototype dwarf nova U Gem (4.25 h). U Gem also shows short and long outbursts with a mean outburst recurrence time of ~ 110 d (Szkody & Mattei 1984), is much longer than V729 Sgr.

The second long outburst is shown in Figure 2. After the initial rise from quiescence, the flux remains roughly constant for nearly 2 days (a feature which we call a ‘plateau’ phase), after which there is a further increase in flux which is the long outburst. In Figure 2 we show this long outburst, superposed with the profiles of the five short outbursts. We have shifted the short outbursts in time by-eye so that each outburst profile has its ‘zero’ point coinciding with the peak of the outburst and the start of the plateau phase of the long outburst. We find that while there is a spread of ~ 10 percent in the average short outburst amplitude, the amplitude and rise time of the short outbursts are very similar to that of the initial rise in the long outburst.

This behaviour is similar to the superoutbursts observed in the SU UMa dwarf novae (which tend to have shorter orbital periods, $\lesssim 2$ h) and the long outbursts seen in U Gem-

type dwarf novae, both types of systems which have been observed in detail using *Kepler* (e.g. V447 Lyr, Ramsay et al. 2012). Indeed, it appears that all super and long outbursts seen in dwarf nova have a short outburst precursor (see Cannizzo 2012). The first long outburst does not show such a clear plateau phase as the second, (perhaps due to residual imperfections in the corrections applied to the raw light curve), but appears to be broadly consistent with such a view.

3 THE ECLIPSE

To investigate the light curve of V729 Sgr in more detail we extracted sections during quiescence and fit each of these with a linear plus Gaussian function. We then took the mid-point of each observed eclipse (the times are given in Appendix 1) and determined a linear fit to these times giving the ephemeris:

$$T_o = BMJD57300.5183(5) + 0.173405(2)E \quad (1)$$

where the numbers in parentheses give the standard error on the last digits. Our determined period, 4.1617 h, is consistent with that found by Cieslinski et al. (2000) and we take this to be the orbital period of V729 Sgr.

We then detrended the light curves covering the short and long outbursts (i.e., the effects of the outbursts have been removed) and determined the time of the eclipses from these data. Taking the individual eclipse times and converting these to orbital phase using equation 1, we find an indication that the mid-point of the eclipse occurs earlier during outburst compared to quiescence. To reduce noise in the eclipse profile, we formed the mean profile using 6–8 eclipses

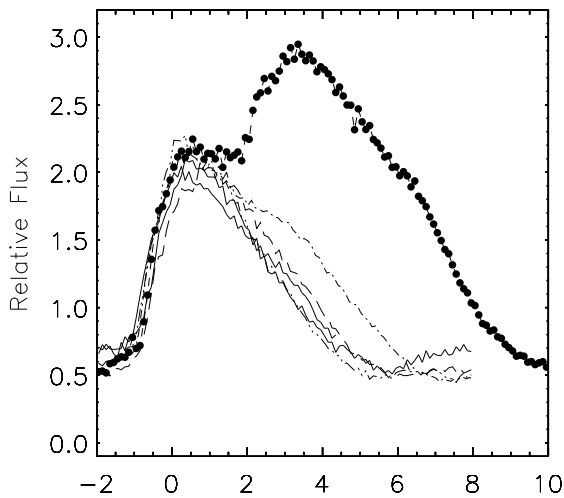


Figure 2. The light curve (black dots) is the second long outburst observed for V729 Sgr using *K2*. The superimposed lines show the five short outbursts where each peak time has been shifted (by eye) to the time zero, matching the start time of the plateau phase.

(the exact number depended on how many eclipses there were between outbursts) and determined the phase of the mid-point of the average eclipse using a linear fit plus Gaussian profile. We show the determined orbital phase of the eclipse over the course of the *K2* observations in the lower panel of Figure 1. We find that the mid-eclipse occurs at an earlier phase during outburst compared to quiescence.

This finding is very similar to our result made using *Kepler* data of the U Gem dwarf nova V447 Lyr (Ramsay et al. 2012) and KIS J192748.53+444724.5 (Scaringi, Groot & Still 2013). During quiescence a significant fraction of the light is emitted from the bright spot where the accretion stream meets the accretion disk around the white dwarf. The bright spot gets eclipsed *after* the white dwarf has been eclipsed. During outburst the contribution of the bright spot to the system brightness is reduced and therefore during outburst the mid-point of the eclipse appears *earlier* compared to during quiescence.

To explore the eclipse profile further, we took the detrended light curves and folded and binned them to give mean orbital curves for quiescence, short outbursts and long outburst and these are shown in Figure 3. The quiescent light curve is very similar to V447 Lyr and shows a peak at $\phi \sim 0.8$ – 0.9 which is due to the bright spot. During short and long outbursts this bright peak, however, is not detected and instead a minimum is seen at $\phi \sim 0.7$ – 0.8 . In addition, the eclipse becomes deeper from quiescence to short outburst and into long outburst, which may indicate that the system brightness is concentrated close to the white dwarf (perhaps the boundary layer between the accretion disk and white dwarf). The eclipse is also broader during outburst and indicates (as was seen in V447 Lyr) that the disk has a greater extent compared to quiescence.

4 SUPERHUMPS

CVs show a range of periodic and quasi-periodic behaviour in their light curves. In the absence of eclipses and/or phase resolved spectra it can sometimes be difficult to determine the origin for periods identified in power spectra. This is due to the fact that in addition to there generally being a signature of the orbital period in the light curve, CVs quite often show signatures of ‘superhumps’. The ‘positive’ superhumps are due to torsional disc oscillations and have periods slightly longer than the orbital period (e.g., Wood et al. 2011), whereas the ‘negative’ superhumps result from a tilt and retrograde precession of the accretion disc (e.g., Wood, Thomas, & Simpson 2009). In the latter case, the accretion stream bright spot transiting the face of the tilted disc provides the negative superhump signal. For CVs with orbital periods shorter than ~ 2 hrs, positive superhumps are seen in almost all CVs found in superoutburst (e.g., Patterson et al. 2005). The ‘period excess’ over the orbital period has been used to estimate the orbital period of many CVs.

There are a small number of CVs where negative superhumps have been detected including during quiescence (e.g. Wood et al. 2011 reported negative superhumps in the *Kepler* observations of V344 Lyr, and Osaki & Kato 2013 reported the detection of negative superhumps over a full supercycle using *Kepler* observations of V1504 Cyg). The physical origin of the tilt of the disk negative superhumps has not been firmly established, but Thomas & Wood (2015) adapted the results of Lai (1999) in smoothed particle hydrodynamic simulations to find that a magnetic field on the primary can tilt the disk out of the orbital plane.

We detrended the light curves for the short and long outburst intervals seen in V729 Sgr and then obtained Lomb Scargle Power Spectra and also Discrete Fourier Transforms (DFT) of these light curves. The short or long outbursts show no evidence for a period in the light curve other than P_{orb} (which we know precisely from the eclipses). However, we find evidence for a period which is shorter than the orbital period in five out of the six quiescent epochs. To investigate this in more detail we pre-whitened the light curves by removing the orbital period and its three harmonics and then obtained a DFT. We show the DFT of the six detrended light curves in Figure 4. These DFT show clear peaks at a period which is shorter than the orbital period in five of the six quiescent light curves: we identify these peaks as a signature of a negative superhump. We indicate the period of these peaks in Table 1 and also the negative superhump excess $\epsilon^- = (P_{orb} - P_{sh})/P_{orb}$. We also did the same analysis using a single light curve made up of the individual detrended Q2-Q6 quiescent light curves, and find a strong peak at 237.4 min. We folded each of the quiescent light curves on the periods shown in Table 5. The mean negative excess, 0.049, is consistent with the relationship between ϵ^- and P_{orb} , derived using 19 CVs in the study of Wood, Thomas & Simpson (2009).

5 DISCUSSION

5.1 General Characteristics

The upper panel of Fig. 1 indicates that V729 Sgr has characteristics which are typical of CVs, showing frequent short

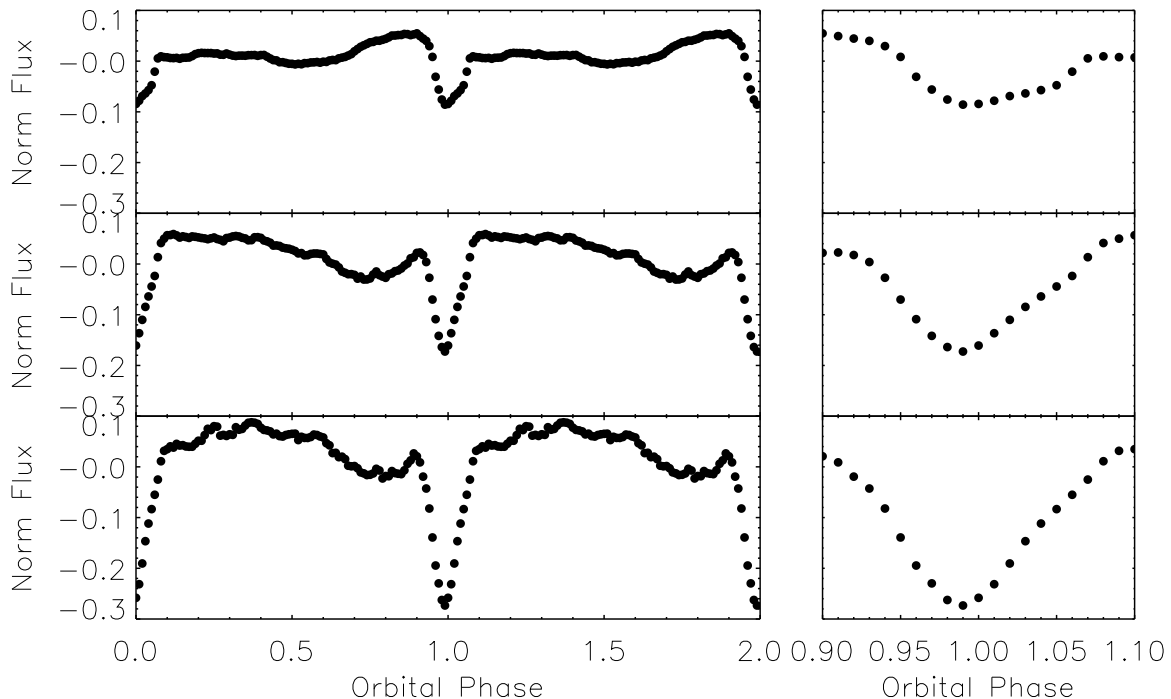


Figure 3. The folded and binned light curves of V729 Sgr during quiescence (top panel); short outburst (middle panel) and long outburst (bottom panel). In the right hand panels we highlight the profile of the eclipse.

Quiescence Section	P_{sh}^- (min)	ϵ^-
Q2	238.18	0.046
Q3	236.30	0.054
Q4	237.46	0.049
Q5	237.60	0.048
Q6	237.31	0.050

Table 1. We show the period identified in each of the six quiescent epochs and indicate whether they are likely negative superhumps (P_{sh}^-) or positive superhumps (P_{sh}^+) and note the positive ϵ^+ and negative ϵ^- super-hump excess.

and long outbursts. The light curve also shows eclipses, allowing the orbital period to be unambiguously determined, (4.16 hr), placing it above the orbital period gap. By determining the phase of the mid-eclipse we find that the eclipse center occurs earlier in phase during an outburst compared to quiescence (lower panel of Fig 1). This is consistent with observations of other CVs, and is due to the differing relative contribution of the bright spot to the overall optical brightness in outburst compared to quiescence. The duration of the short outbursts seen in V729 Sgr are also typical of sources with similar orbital period, whilst the duration of the long bursts are marginally shorter (we caution that we have a sample of only two long outbursts) than other CVs with similar orbital period (see Fig 17 and 18 of Otulakowska-Hypka et al. 2016).

5.2 The frequency of outbursts

However, there are two features of the *K2* light curve of V729 Sgr which make this CV rather unusual. The first is the high frequency of the outbursts, which is ~ 10 d for successive short outbursts and 38 d between the two long outbursts (which by necessity we assume is typical of the rate of long outbursts in this system). In Figure 6 we plot the recurrence times of short and long outbursts for the 17 CVs with values reported in Ritter & Kolb (2003) (all systems have an orbital period less than 2.1 hrs) and we add the values for V729 Sgr and V447 Lyr (Ramsay et al. 2012). The general trend, which was noted by Warner (1995), is that the short outburst rate is proportional to the super or long outburst rate.

The *Kepler* observations of V447 Lyr (orbital period 3.74 hr) show it is only a marginal outlier compared to the short period systems, but V729 Sgr is clearly an outlier and falls into the lower left of Fig 2 of Warner (1995), which has only 3 systems in this part of the distribution. These systems are the ER UMa systems (a sub-class of CVs which also includes V1159 Ori and RZ LMi, see Kato et al. 2016) which show outbursts every handful of days and superoutbursts every month or so. This is unexpected (and so far not adequately explained) since a short recurrence time is predicted to be due to a high mass accretion rate. However, the known ER UMa CVs all have periods below the orbital period gap at 2 hrs (RZ LMi has an orbital period of ~ 83 min) and are therefore expected to have relatively low mass transfer rates. In the case of V729 Sgr we have a CV above the period gap (and hence higher mass transfer rate) which shows frequent outbursts.

Dwarf novae exhibit a considerable scatter in outburst properties at a given orbital period (Patterson 1984, Knigge

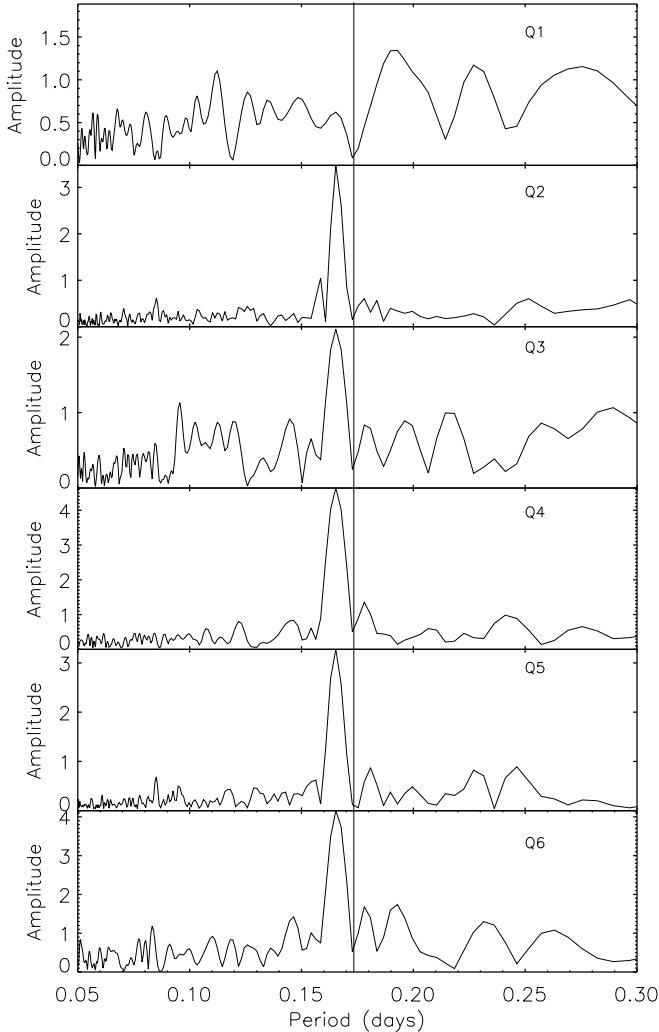


Figure 4. We show the Discrete Fourier Transform of the six quiescent light curves of V729 Sgr where we have first detrended the data and also pre-whitened the light curve using the orbital period and its three harmonics. The vertical line indicates the orbital period. The Q2–Q6 data indicate the presence of a negative super-hump.

et al. 2011), indicating the mass transfer rate \dot{M}_T feeding into the outer disk can vary considerably from one system to another. This is presumably due to the fact that the secondary stars can have widely varying histories to end up at a given orbital period, as evidenced by the dispersion in stellar radii at given orbital period (Knigge et al. 2011; see their Figure 6). In the disk instability model, higher \dot{M}_T translates into a faster build-up of accretion disk material in quiescence, and therefore more frequent outbursts. Therefore V729 Sgr can be explained by invoking a higher-than-average \dot{M}_T .

Superoutbursts are usually defined as long outburst exhibiting (positive) superhumps, and yet in V729 they are lacking. Our current understanding for superhumps is that they are due to a torsionally oscillating eccentric disk which undergoes prograde precession (Whitehurst 1988). Physical conditions in the disk allow for this to occur when the

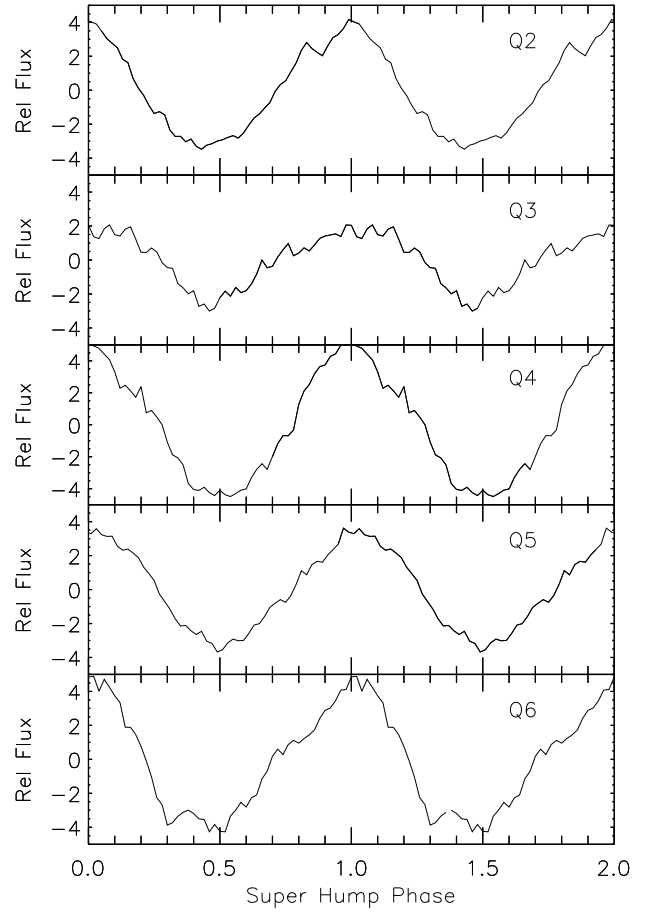


Figure 5. For the five quiescent time intervals which show evidence of superhumps we folded and binned the detrended and prewhitened (on the orbital period and three harmonics) light curves on the period shown in Table 1. We have phased the data so that flux maximum is defined as $\phi=0.0$ and we have plotted the folded light curve twice so that it runs from 0.0–2.0.

disk grows large enough so that the radius of 3:1 resonance with the binary orbital period is exceeded. Given that CV primary masses are $\sim 1M_\odot$ and the secondary mass is $\sim 0.1M_\odot (P_{\text{orb}}/1 \text{ hr})$, this means superhumps can only occur in short orbital period systems $P_{\text{orb}} < 3 \text{ hr}$. The mass ratio in V729 is probably not extreme enough to support superhumps during outburst because the point of 3:1 resonance lies beyond the last stable (i.e., non-intersecting) orbit. Van Paradijs (1983) carried out a study of long and short outbursts above and below the 2–3 hr period gap and concluded that superoutbursts in the SU UMa systems are consistent in their properties with long outbursts in systems above the period gap. In other words, dwarf novae in general exhibit alternating series of long and short outbursts. Systems below the period gap tend to have more short outbursts between two long outbursts. The lack of superhumps in the long outbursts in V729 Sgr and V447 Lyr indicates they are not required for long outbursts to occur.

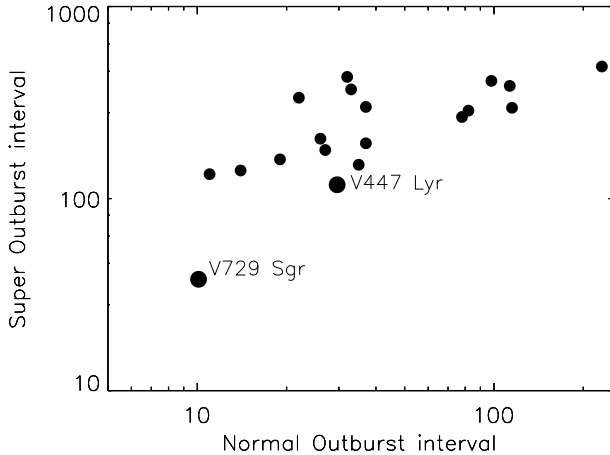


Figure 6. We show the relationship between the outburst interval for short and super/long outbursts in CVs where we have taken the data from Ritter & Kolb (2003). The source with the longest orbital period of 2.1 hrs. We have placed the location of V729 Sgr using the results from the K2 data.

5.3 The detection of negative superhumps

The second feature of V729 Sgr which make it unusual is the presence of negative superhumps during quiescence. Wood et al. (2009) list 21 CVs which have negative super-hump excesses reported in the literature. The system with the longest orbital period was TV Col which has a moderately magnetic white dwarf (and is an intermediate polar). The next longest period system was LT Eri (SDSS J0407-0644) with $P_{orb}=4.08$ hrs. The Ritter & Kolb Catalogue 7.23 (2015 Dec) (Ritter & Kolb 2003) gives 27 sources which are reported as displaying negative superhumps. Three have orbital periods longer than V729 Sgr. AT Cnc ($P_{orb}=4.83$ h was reported to have negative superhumps with $P_- = 4.65$ h and 4.74 h made when it was in a bright standstill episode (Kozhevnikov 2004). Quasi-Periodic signals were seen in AY Psc ($P_{orb}=5.22$ h) over three years which were ~ 5 percent shorter than P_{orb} (Gülsecen et al. 2009) and interpreted as negative superhumps (it is unclear whether these superhumps were seen in quiescence or outburst). Finally, KIC 9406652 ($P_{orb}=6.11$ h) was found to show a period of 5.75 hr (Gies et al. 2013) which although present over the whole of the *Kepler* observations its amplitude varied over time, making KIC 9406652 the longest period CV to show negative superhumps. V729 Sgr is therefore unusual (although not unique) in showing negative superhumps above the orbital period gap during quiescence.

6 CONCLUSIONS

V729 Sgr is worthy of further investigation since it shows outbursts on a more frequent basis than its orbital period indicates. Future observations should set out to identify further examples of long outbursts and determine their frequency. Higher cadence observations are encouraged at all accretion states to search for superhumps (both positive and negative) to determine how often the negative superhumps are observed in this system. It should shed important light

on the nature of accretion disks in high mass transfer rate systems.

7 ACKNOWLEDGMENTS

We thank Andrew Vanderburg for supplying us with the SC K2 light curve of V729 Sgr. Armagh Observatory is supported by the Northern Ireland Government through the Dept for Communities. This material is based upon work supported by the National Science Foundation under Grant No. AST-1305799 to Texas A&M University-Commerce.

REFERENCES

- Cannizzo J. K., 2012, ApJ, 757, 174
 Cieslinski D., Steiner J. E., Pereira P. C. R., Pereira M. G., 2000, PASP, 112, 349
 Dai Z., Szkody P., Garnavich P. M., Kennedy M., 2016, AJ, 152, 5
 Ferwerda J. G., 1934, BAN, 7, 166
 Gies D. R., Guo Z., Howell S. B., Still M. D., Boyajian T. S., Hoekstra A. J., Jek K. J., LaCourse D., Winarski, T., 2013, ApJ, 775, 64
 Gülsecen H., Retter A., Liu A., Esenoglu H., 2009, NewA, 14, 330
 Kato T. et al., 2016, PASJ, 68, 107
 Kennedy M. R., Garnavich P., Breedt E., Marsh T. R., Gänsicke B. T., Steeghs D., Szkody P., Dai Z., 2016, MNRAS, 459, 3622
 Knigge C., Baraffe I., Patterson J., 2011, ApJS, 194, 28
 Kozhevnikov V. P., 2004, A&A, 419, 1035
 Howell, S. B., et al., 2014, PASP, 126, 398
 Lai, D. 1999, ApJ, 524, 1030
 Osaki Y., Kato T., 2013, PASJ, 65, 50
 Otulakowska-Hypka M., Olech A., Patterson J., 2016, MNRAS, 460, 2526
 Patterson J., 1984, ApJS, 54, 443
 Patterson J., et al., 2005, PASP, 117, 1204
 Ramsay G., Cannizzo J. K., Howell S. B., Wood M. A., Still M., Barclay T., Smale A., 2012, MNRAS, 425, 1479
 Ritter H., Kolb U., 2003, A&A, 404, 301
 Scaringi S., Groot P. J., Still M., 2013, MNRAS, 435, L68
 Szkody P., Mattei J. A., 1984, PASP, 96, 988
 Thomas, D. M., & Wood, M. A. 2015, ApJ, 803, 55
 Vanderburg A., Johnson J. J., 2014, PASP, 126, 948
 Van Cleve J. E., Howell S. B., Smith J. C., Clarke B. D., Thompson S. E., Bryson S. T., Lund M. N., Handberg R., Chaplin W. J., 2016, PASP, 128, 5002
 Van Paradijs J., 1983, A&A, 125, L16
 Warner B., 1995, ApSS, 226, 187
 Whitehurst R., 1988, MNRAS, 232, 35
 Wood M. A., Thomas D. M., Simpson J. C., 2009, MNRAS, 398, 2110
 Wood M. A., Still M. D., Howell S. B., Cannizzo J. K., Smale A. P., 2011, ApJ, 741, 105

APPENDIX A: ECLIPSE TIMES

Table A1. The time of the mid-eclipse (BMJD) is shown with the cycle number in the right hand column (see §3 for details).

Time (BMJD)	Cycle	Time (BMJD)	Cycle	Time (BMJD)	Cycle
57309.540	52	57338.492	219	57375.430	432
57309.707	53	57338.668	220	57375.605	433
57309.880	54	57338.840	221	57375.777	434
57310.050	55	57339.016	222	57375.940	435
57310.227	56	57339.188	223	57376.130	436
57310.406	57	57339.360	224	57376.300	437
57310.574	58	57346.645	266	57376.470	438
57310.746	59	57346.816	267	57376.640	439
57310.926	60	57346.992	268		
57311.094	61	57347.164	269		
57311.270	62	57347.336	270		
57311.445	63	57347.510	271		
57311.613	64	57347.684	272		
57311.790	65	57347.855	273		
57311.965	66	57348.030	274		
57312.137	67	57348.203	275		
57323.586	133	57348.380	276		
57323.750	134	57348.550	277		
57323.930	135	57348.900	279		
57324.100	136	57349.070	280		
57324.277	137	57349.242	281		
57324.453	138	57349.420	282		
57324.620	139	57349.594	283		
57324.797	140	57349.770	284		
57324.970	141	57349.940	285		
57325.140	142	57362.074	355		
57325.316	143	57362.250	356		
57325.490	144	57362.420	357		
57325.660	145	57362.600	358		
57325.840	146	57362.777	359		
57326.010	147	57362.950	360		
57326.180	148	57363.117	361		
57326.355	149	57363.290	362		
57326.527	150	57363.465	363		
57326.703	151	57363.637	364		
57326.875	152	57363.812	365		
57327.047	153	57363.984	366		
57327.223	154	57364.156	367		
57327.395	155	57364.332	368		
57327.570	156	57364.504	369		
57327.742	157	57364.676	370		
57327.914	158	57364.850	371		
57328.090	159	57365.023	372		
57328.260	160	57365.195	373		
57328.438	161	57365.370	374		
57328.610	162	57365.543	375		
57328.785	163	57365.720	376		
57328.957	164	57365.890	377		
57336.418	207	57366.070	378		
57336.586	208	57366.242	379		
57336.766	209	57373.690	422		
57336.934	210	57373.867	423		
57337.105	211	57374.043	424		
57337.280	212	57374.215	425		
57337.453	213	57374.387	426		
57337.625	214	57374.562	427		
57337.797	215	57374.740	428		
57337.977	216	57374.906	429		
57338.145	217	57375.082	430		
57338.320	218	57375.258	431		